Accelerated deep learning-based estimation of wavefront dips and curvatures and their application to 3D prestack data enhancement

Kirill Gadylshin, IPGG SB RAS, Novosibirsk State University; Ilya Silvestrov and Andrey Bakulin, EXPEC Advanced Research Center, Saudi Aramco*

Summary

We present a novel workflow for the accelerated signal enhancement of massive 3D prestack seismic data utilizing a Local Wavefront Attributes Deep Neural Network. It is based on automatic local wavefront attributes estimation using a specially trained convolutional deep neural network. The general workflow is adaptive to a particular 3D prestack seismic volume. It requires performing a conventional semblance-based estimation of wavefront dips and curvatures for only about 1% of the whole amount of data. The verification of the proposed approach is done on challenging real datasets, both marine and land. Deep learning allows achieving a significant speed-up compared to the conventional method while preserving an acceptable quality of the results.

Introduction

Kinematic wavefront attributes form a foundation of many seismic data processing methods. The first-order traveltime derivatives are used in slope- or stereo-tomography methods (Lambaré, 2008; Bakulin et al., 2021a) to estimate depth velocity models. Curvatures of normal and normal-incidence-point wavefronts at zero offset are used in the common-reflection-surface (CRS) method to produce stacking seismic sections with an improved signal-to-noise ratio (Mann et al., 1999). A general representation of the local stacking operators as second-order traveltime approximations were used by Hoecht et al. (2009) to interpolate seismic data. Bakulin et al. (2020) developed nonlinear beamforming (NLBF) technique to efficiently enhance massive 3D prestack land seismic data targeting imaging and near-surface applications. Estimating the kinematic attributes is usually the most computationally demanding part of most data processing algorithms discussed above. In addition, their recomputation might be performed many times at different stages, such as in adaptive multi-scale processing (Bakulin et al., 2019).

Recently, a strong interest in machine learning-based approaches has emerged in seismic data processing and interpretation (Yu and Ma, 2021). One of the abiding tasks in exploration geophysics is the denoising problem. Zhu et al. (2019) used DeepDenoiser neural network to separate noise and signal by learning a nonlinear regression. Kaur et al. (2020) proposed a CycleGAN algorithm to suppress ground roll. A physics-constrained solution based on a combination of unsupervised and supervised deep learning approaches for ground roll attenuation was proposed by Pham and Li (2022). In seismic interpretation, the localization of faults, dips, and layers is similar to object detection problems in computer vision. Deep neural networks for image classification are used in seismic attributes analysis (Das et al., 2019). Zu et al. (2021) and Huang et al. (2021) presented approaches for local slope estimation by convolutional neural networks directly from the prestack data. Gadylshin et al. (2020) proposed the accelerated estimation of local wavefront attributes, including curvatures, utilizing a partially convolutional neural network.

The direct calculation of local dips only using a Local Wavefront Attributes Deep Neural Network (LWA DNN), was developed by Gadylshin et al. (2021). In this study, we extend the LWA DNN workflow for simultaneous estimation of dips and curvatures, used in the NLBF method for prestack data enhancement. In addition, we demonstrate how transfer learning can be applied to eliminate or reduce the turnaround time associated with additional training of the neural network.

Method

In the NLBF method, we assume that traveltime surface can be approximated with local moveout, used in beamforming, as follows:

$$\Delta t = A\Delta x + B\Delta y + C\Delta x\Delta y + D\Delta x^2 + E\Delta y^2,$$

where A, B, C, D, E are unknown local wavefront attributes, Δx and Δy represent spatial shifts of the summed trace with respect to the output trace (for more details, see Bakulin et al., 2020). The unknown coefficients A, B (wavefront first spatial derivatives, or dips) and C, D, E (wavefront second derivatives, or curvatures) are estimated by probing many different beamforming surfaces and picking one with the best coherency defined by the maximum value of a specified semblance function S. Typically, wavefront attributes are estimated on a dense regular spatial and temporal grid. The standard estimation approach has the semblance optimization procedure at the core. Therefore, the costly optimization task must be solved at each dense 3D X-Y-T grid point. Following Gadylshin et al. (2021), we suggest using the LWA DNN to get around the expensive, standard workflow. In this study, we extend this workflow to simultaneously reconstruct dips, curvatures, and semblance.

Considering the hybrid "2+2+1" estimation strategy (Bakulin et al. 2021b), one first searches for the A and D

parameters in the $X-T$ plane, then B and E in the $Y-T$ plane, while the last parameter, C, is evaluated in the end. In the LWA DNN workflow, we follow a similar sequence – the corresponding dip and curvature pairs in $X-T$ (A and D) or $Y-T$ (B and E) plane are simultaneously estimated using only the "flat" image of the data,. i.e., using 2D cross-sections of the seismic data extracted from 3D volume. In the current implementation, the C attribute's estimation is out of the scope of DNN workflow, and we assign its value to zero.

Let us explain the training dataset generation in more detail. For clarity, let us illustrate the new methodology only using one plane containing the X-axis direction. Same approach is valid for another plane containing the Y-axis (one needs to interchange the X variable with the Y variable and A and D attributes pair with the B and E attributes pair). For each time-space coordinates *(t, x)*, we transform a triplet of multi-parameter attributes < A, D, S> into a <Red, Green, Blue> (RGB) color image pixel. To obtain the corresponding seismic data on the regular grid, consistent with the output attributes grid, we perform the supergrouping-based preprocessing step (see Gadylshin et al., 2021). The example of the LWA DNN training data is shown in Figure 1.

The proposed LWA DNN workflow aims to obtain local wavefront attributes directly from the data by replacing resource-intensive semblance-based computations of conventional NLBF estimation procedures with DNN prediction. The first step is to perform attributes estimation using the conventional brute-force semblance optimization approach on only 1% of prestack data followed by subsequent conversion of estimated dips, curvatures, and semblance to colored RGB images. The second step performs regularization of the prestack data, thus finalizing the creation of the representative training dataset. The third step is the LWA DNN training and verification. Finally, we predict the remaining 99% of local wavefront attributes and convert them from RGB images to physical values.

Marine data example: signal enhancement via nonlinear beamforming

We consider marine Ocean-Bottom Cable (OBC) 3D seismic data in our first numerical experiment. We employ the LWA DNN to this dataset for dips and curvature prediction with the subsequent nonlinear beamforming (NLBF) application for data enhancement before FWI.

The data were acquired with 100 x 50 m shot spacing and 50 x 300 m OBC receiver spacing in inline and crossline directions, respectively. The studied survey area is 3.5 x 43 km, containing six receiver lines with 240 active channels and 500 shot crosslines with 72 shots positions on each. The listening time is 7 s and sample interval is 4 ms. The data is sorted in the cross-spread domain and contains 3252 cross-spread gathers. At the first stage of our workflow, we perform a conventional estimation of local wavefront attributes based on brute-force semblance optimization technique using only 1% of all cross-spread gathers (Figure 2). We then convert estimated dips, curvatures, and semblance to the colored RGB images. Following the LWA DNN workflow, we apply

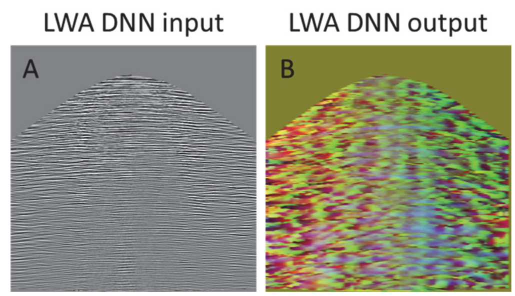

Figure 1: The training data example. After regularization, the input seismic data was converted to a 512x512 grayscale image (A). The corresponding encoded local wavefront attributes were estimated using conventional semblance-based optimization and converted to an image (B).

supergrouping-based regularization to obtain data on a regular grid with enhanced SNR. Next, LWA DNN training and verification are performed. In this experiment, the training process took ~600 s on a single GPU node with four NVIDIA Tesla P100. The DNN-predicted attributes show a

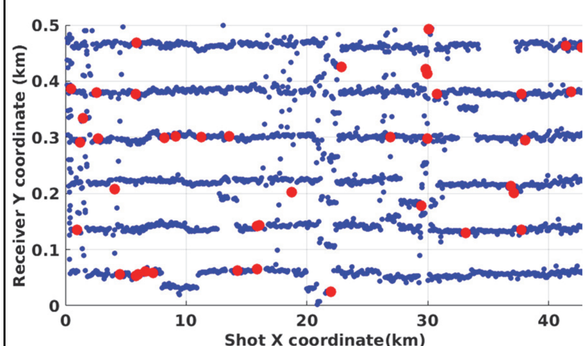

Figure 2. The acquisition's cross-spread centers of the marine OBC dataset are plotted as blue points in the shot-X/receiver-Y domain. Red points indicate the positions of the selected cross-spreads used for LWA DNN training.

reasonable match with the conventional method (Figure 3). An average estimation time using conventional technique took about 1300s on a single dual socket CPU node based on 16 core Intel Haswell processors. The LWA DNN prediction time for one cross-spread gather took about 3 s.

The attributes estimation is an intermediate step in the NLBF method; therefore, it is essential to evaluate the influence of the predicted attributes on the beamforming results. To do so, we compare the raw data after one of the processing stages (Figure 4a), with the additional data enhancement using conventional NLBF (Figure 4b) and AI-assisted NLBF (Figure 4c). The difference between the two enhancement scenarios is reasonably small (Figure 4e). It demonstrates the ability of LWA DNN to efficiently predict the local wavefront attributes skipping the tedious semblance-based estimation approach.

Transfer learning example: application of pre-trained LWA DNN to real land seismic data

Finally, let us apply LWA DNN, pre-trained on OBC marine data, to the land seismic data enhancement. We consider land seismic data acquired with 72-geophones arrays and five vibrators per sweep in a challenging desert environment with low SNR. The data have been passed through a standard processing workflow, including denoising steps with high-amplitude and linear-noise attenuation (Figure 5a). Despite the significant effort in processing, reflected waves remain largely invisible. First, we apply standard NLBF enhancement to a single test cross-spread gather (Figure 5b). The estimation time on a single CPU node is about 830 s.

The transfer learning approach allows even more tremendous speed-up of the calculations since no additional training is required, whereas the LWA DNN weights estimated in the OBC marine data are utilized. In this experiment, we are less concerned about the exact accuracy of estimated kinematic attributes. Instead, we focus on enhanced data itself as a processing deliverable. We may always perform additional limited training to improve the LWA DNN prediction quality if required. The comparison of conventional and AI-assisted NLBF (with transfer learning) is presented in Figure 5. The final enhanced prestack data appear very similar (see the difference, plotted using the same scale, Figure 5d). Comparing the original data after the standard processing (Figure 5a) and the final AI-assisted NLBF results (Figure 5c), we conclude that in this particular example, one may skip a time-consuming generation of the training dataset and additional training of LWA DNN, since transfer learning delivers results acceptable for processing. The estimation time using the LWA DNN on a test cross-spread is about 3 s, which is two orders of magnitude less than the conventional NLBF.

Conclusions

We presented a novel DNN-based workflow for the accelerated enhancement of massive 3D prestack seismic data. It is based on automatic local wavefront attributes estimation utilizing a specially trained convolutional deep neural network called LWA DNN. In the new implementation, both dips and curvatures of the wavefront are simultaneously estimated. Although this workflow is adaptive to a particular 3D prestack seismic volume, we also presented a transfer learning experiment with challenging land seismic data acquired in a desert environment. We used the LWA DNN pre-trained on a massive 3D marine OBC dataset in this experiment. In both cases (without and with transfer learning), we significantly sped up the NLBF signal enhancement procedure. However, we save the computational time in the transfer learning experiment by bypassing the representative training dataset generation and LWA DNN additional training. In our future investigations, we plan to assess different transfer learning strategies (both with and without additional limited training) and try to find the optimal trade-off between the quality of the enhanced data and AI-assisted NLBF performance.

Acknowledgments

One of the authors (Kirill Gadylshin) was supported by RSF grant No. 22-21-00738.

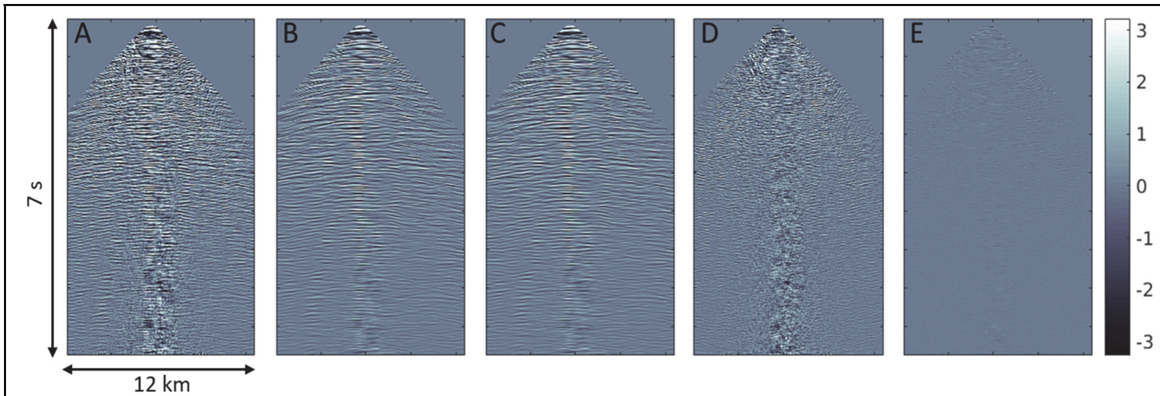

Figure 4: Prestack marine OBC data before and after enhancement: (a) input data at one of the processing stages after NMO correction; (b) same but after conventional NLBF; (c) after application of AI-assisted NLBF; (d) noise removed by conventional NLBF (difference between (a) and (b)); (e) the difference between gathers enhanced with conventional (b) and AI-assisted NLBF (c).

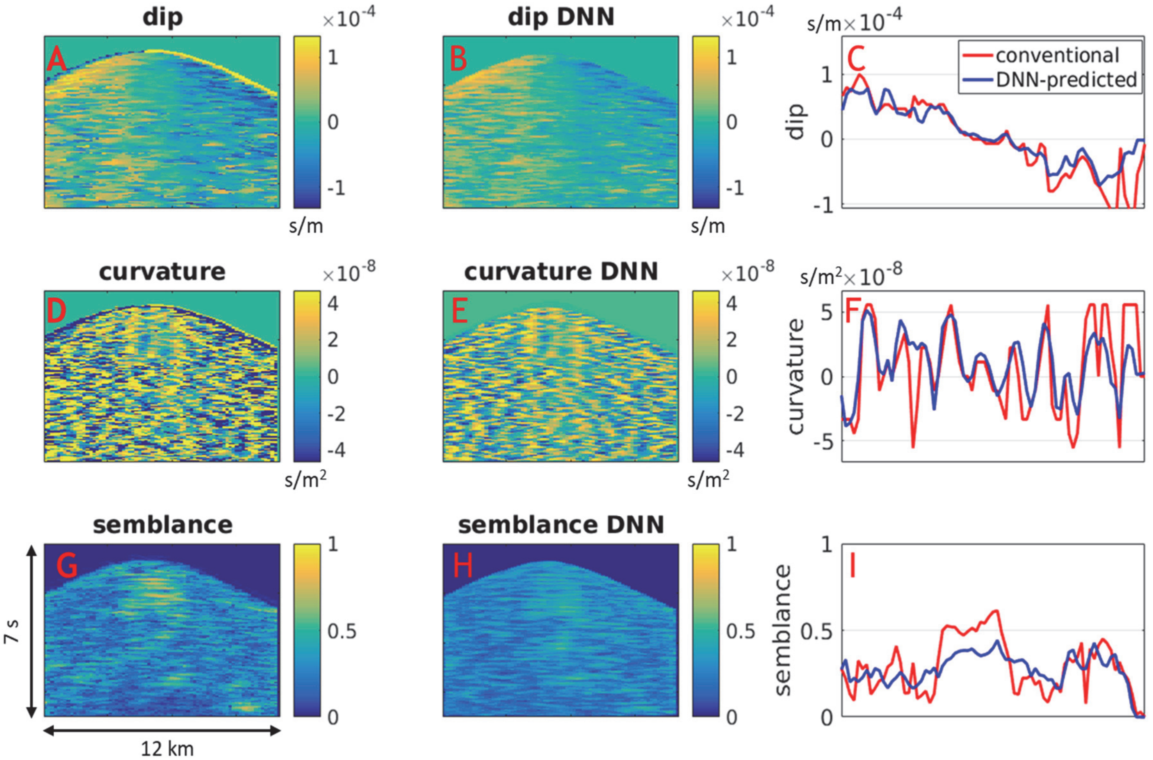

Figure 3. Example of attributes prediction by LWA DNN for the 3D marine OBN dataset. The conventionally estimated dips (A), curvatures (D), semblance (G), and the DNN-predicted dips (B), curvature (E), semblance (H). The right column shows the horizontal profiles (at t=2.5 s) comparing conventionally estimated (red), and DNN-predicted (blue) attributes: dips (C), curvatures (F), and semblance (I).

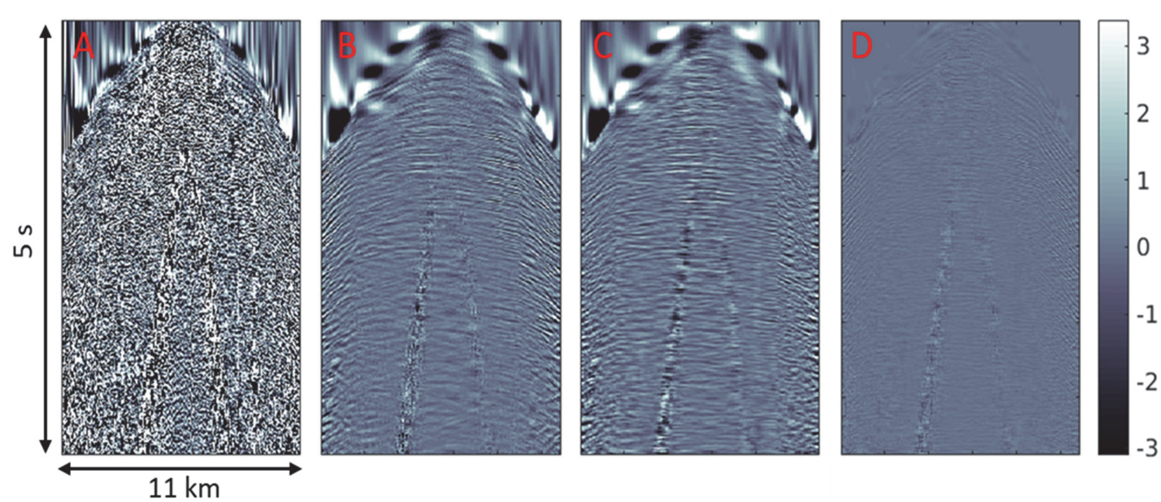

Figure 5: Prestack land data before and after enhancement: (a) input data; (b) after application of conventional NLBF; (c) after application of AI-assisted NLBF; (d) the difference between gathers enhanced using conventional (b) and AI-assisted NLBF (c).

REFERENCES

Bakulin, A., P. Golikov, M. Dmitriev, D. Neklyudov, P. Leger, and V. Dolgov, 2018, Application of supergrouping to enhance 3D prestack seismic data from a desert environment: The Leading Edge, **37**, 200–207, doi: https://doi.org/10.1190/tle37030200.1.

Bakulin, A., I. Silvestrov, and M. Dmitriev, 2019, Adaptive multi-scale processing of challenging 3D seismic data for first-break picking, FWI and imaging: 89th Annual International Meeting, SEG, Expanded Abstracts, 3979–3984, doi: https://doi.org/10.1190/segam2019-3214616.1.

Bakulin, A., I. Silvestrov, M. Dmitriev, D. Neklyudov, M. Protasov, K. Gadylshin, and V. Dolgov, 2020, Nonlinear beamforming for enhancement of 3D prestack land seismic data: Geophysics, **85**, no. 3, V283–V296, doi: https://doi.org/10.1190/geo2019-0341.1.

Bakulin, A., I. Silvestrov, D. Neklyudov, K. Gadylshin, and M. Protasov, 2021a, 3D data-domain reflection tomography for initial velocity model building using challenging 3D seismic data: Journal of Seismic Exploration, **30**, 419–446.

Bakulin, A., I. Silvestrov and M. Protasov, 2021b, Evaluating strategies for estimation of local kinematic parameters in noisy land data: quality versus performance trade-offs: Journal of Geophysics and Engineering, **18**, 890–907, doi: https://doi.org/10.1093/jge/gxab060.

Das, V., A. Pollack, U. Wollner, and T. Mukerji, 2019, Convolutional neural network for seismic impedance inversion: Geophysics, **84**, no. 6, R869–R880, doi: https://doi.org/10.1190/geo2018-0838.1.

Gadylshin, K., I. Silvestrov, and A. Bakulin, 2020, Inpainting of local wavefront attributes using artificial intelligence for enhancement of massive 3-D prestack seismic data: Geophysical Journal International, **223**, 1888–1898, doi: https://doi.org/10.1093/gji/ggaa422.

Gadylshin, K., I. Silvestrov, and A. Bakulin, 2021, Direct estimation of local wavefront attributes using deep learning: First International Meeting for Applied Geoscience & Energy, SEG/AAPG, Expanded Abstracts, 1596–1600, doi: https://doi.org/10.1190/segam2021-3583265.1.

Hoecht, G., P. Ricarte, S. Bergler, and E. Landa, 2009, Operator-oriented interpolation: Geophysical Prospecting, **57**, 957–979, doi: https://doi.org/10.1111/j.1365-2478.2009.00789.x.

Huang, W. L., F. Gao, and J. P. Liao, 2021, A deep learning network for estimation of seismic local slopes: Petroleum Science, **18**, 92–105, doi: https://doi.org/10.1007/s12182-020-00530-1.

Kaur, H., S. Fomel, and N. Pham, 2020, Seismic ground-roll noise attenuation using deep learning: Geophysical Prospecting, **68**, 2064–2077, doi: https://doi.org/10.1111/1365-2478.12985.

Lambaré, G., 2008, Stereotomography: Geophysics, **73**, no. 5, VE25–VE34, doi: https://doi.org/10.1190/1.2952039.

Mann, J., R. Jäger, T. Müller, G. Höcht, and P. Hubral, 1999, Common reflection-surface stack: A real data example: Journal of Applied Geophysics, **42**, 301–318, doi: https://doi.org/10.1016/S0926-9851(99)00042-7.

Pham, N., and W. Li, 2022, Physics-constrained deep learning for ground roll attenuation: Geophysics, **87**, no. 1, V15–V27, https://doi.org/10.1190/geo2020-0691.1.

Yu, S., and J. Ma, 2021, Deep learning for geophysics: Current and future trends: Reviews of Geophysics, **59**, e2021RG000742, doi: https://doi.org/10.1029/2021RG000742.

Zhu, W., S. M. Mousavi, and G. C. Beroza, 2019, Seismic signal denoising and decomposition using deep neural networks: IEEE Transactions on Geoscience and Remote Sensing, **57**, 9476–9488, doi: https://doi.org/10.1109/TGRS.2019.2926772.

Zu, S., J. Cao, and X. Jiang, 2021, Slope estimation by convolutional neural networks: 82nd Conference and Exhibition, EAGE, Extended Abstracts, doi: https://doi.org/10.3997/2214-4609.202010260.